A corotating two-roll mill for studies of two-dimensional elongational flows with vorticity

Marco A. H. Reyes and Enrique Geffroy[a)]
Instituto de Investigaciones en Materiales, Universidad Nacional Autónoma de México, Apdo. Postal 70-360, Cd. Universitaria, 04510 México, D. F., México

(Received 30 November 1999; accepted 13 June 2000)

A closed-form analytical solution for the Stokes flow generated by a corotating two-roll mill is used to generate two-dimensional elongational flows with well-defined amounts of vorticity. These flow devices can generate conditions found between simple shear and purely elongational flows, and are among the few systems that can take into account the presence of nearby boundaries. In the laboratory, these devices have been used for studies of the microstructural dynamics of complex fluids such as polymeric solutions, colloids, bubbles and drops, etc., and allow pointwise optical studies of the flow parameters. Hence, a comparison is presented of available experimental and numerical results for the stagnation point versus the analytical solution presented here. Based upon this solution, a new design for the two-roll mill is presented for the purpose of minimizing the disadvantages of current mills. © *2000 American Institute of Physics.* [S1070-6631(00)00510-9]

I. INTRODUCTION

For studies in fluid mechanics of non-Newtonian fluids,[1,2] chaotic advection,[3,4] drop and bubble dynamics,[5,6] and many industrial applications (see, e.g., Stone[6]), the use of laminar flows capable of inducing significant deformation on the fluid or the embedded objects are a necessary tool. In general, these flows are needed to study fluid systems that show a marked nonlinear, hysteretic behavior due to its *microstructure*. Simple viscometric flows and purely extensional flows (see, e.g., Ref. 7) are among the two most frequently used flow fields that are kinematically different. On the one hand, viscometric flows have significant amounts of vorticity, and are not expected to produce large deformations on an embedded object; thus, they are classified as *weak flows*. The observed behavior in viscometric steady flows is understood by parcels of fluid that at any given time separate linearly in time (at most, the separation can only grow algebraically); hence, these flows produce only a moderate change on the fluid structure. On the other hand, for steady extensional flows there is no vorticity and two neighboring elements of fluid separate in time *exponentially*; given enough time, the flow induces significant changes on the microstructure of the fluid regardless of its relaxation mechanisms; therefore, these are *strong flows*.[8,9]

The purpose of this paper is to present a flow device capable of significant modification of the microstructure of the fluid: the *two-roll mill*. First, the Fourier series expansion for the Stokes solution is presented, followed by the analytical results for the two most important flow parameters. Then, a comparison of the theoretical predictions of this model versus the experimental and numerical results, available for the region about the stagnation point, is given. Finally, the exact solution is used to propose and predict the behavior of a new configuration for experimental two-roll mills that should be useful for experimental studies of complex fluids.

II. STOKES' SOLUTION FOR THE TWO-ROLL MILL

The two-roll mill consists of two cylinders of equal radii, with collinear axes, and separated by a small distance. This flow cell is based on a new analytical solution that assumes a steady, two-dimensional flow as if generated by rollers of infinite length and rotating with equal angular velocities.[10] Inertial terms are considered negligible. For corotating two-roll mills, there exists a *stagnation point* on the line between the cylinders' axes, with local kinematic conditions characteristic of *elongational flow with some vorticity*.[1] Hence, some of the features of the elongational flow field generated by these mills are as follows.[10] (a) The flow parameters are defined only by the mill's geometry, with the shear rate and the ratio of magnitudes of the rate of deformation tensor to its vorticity prescribed independently. (b) Although these flows belong to the family of *strong flows*, simple shear flows can be approached as closely as needed, increasing monotonically the vorticity. (c) The analytical solution takes into account the presence of the cylinders' boundaries, in contrast with other strong flows used to study long-term effects in embedded objects, such as four-roll mills.[5]

Bipolar cylindrical coordinates (α,β) have been theoretically[11] and experimentally used to study other mills. In 1922, Jeffery[12] presented a solution for the Stokes flow inside the annular region of eccentric cylinders, where the stream function satisfies the biharmonic equation. Two-roll mills with identical cylinders are described by constant values of $\alpha = \pm \alpha_R$, with α being the tangential coordinate, and β being the normal coordinate to the cylinders. The geometric aspects are defined by

$$\frac{g}{2R} = \cosh \alpha_R - 1, \quad d = R \sinh \alpha_R, \tag{1}$$

a)Electronic mail: geffroy@servidor.unam.mx

where g is the gap between rollers, R the cylinders' radii, and $2d$ the distance between points $\alpha=\pm\infty$. The stream function used here is the Fourier series expansion proposed by Jeffery[12] for a bounded domain, but supplemented with a logarithmic term so that the flow at infinity is stationary, and the vortices coincide with the center of the rollers.[13] For two-roll mills with equal cylinders rotating at equal speeds (and located over the y axis), the dynamic no-slip tangential velocity component on cylinders implies $u_\alpha(\pm\alpha_R)=\omega R$, and the normal velocity component being zero requires $u_\beta(\pm\alpha_R)=0$. At infinity the fluid must remain at rest and $\psi(\alpha\to 0,\beta\to 0)=0$. The number of unknowns is always greater by one than the number of equations; therefore, an arbitrary value for the stream function on the cylinders is set by the computation defining a relative value for the rollers' angular speed. A closed-form solution is obtained once the latter constraints are used (see Ref. 10).

The solution for this Stokes flow is given by

$$\frac{\psi}{h}=A_0\cosh\alpha+D_0\alpha\sinh\alpha+K\left(b_0+b_1\cos\beta+\sum_{n=2}^{\infty}b_n\cos n\beta\right)+\sum_{n=1}^{\infty}\left[A_n\cosh(n+1)\alpha+B_n\cosh(n-1)\alpha\right]\cos n\beta, \tag{2}$$

where

$$b_0=a_0\cosh\alpha-\frac{a_1}{2},\quad b_1=a_1\cosh\alpha-a_0-\frac{a_2}{2}, \tag{3a}$$

$$b_n=a_n\cosh\alpha-\frac{a_{n+1}}{2}-\frac{a_{n-1}}{2}, \tag{3b}$$

and

$$a_0=\alpha-\ln 2,\quad a_n=-2\exp(-n\alpha)/n. \tag{4}$$

The remaining coefficients A_0, A_1, B_1, D_0, A_n, and B_n are given, respectively, by

$$A_0=\frac{2R\omega\alpha_R\sinh\alpha_R-2K[b_0(\sinh\alpha_R+\alpha_R\cosh\alpha_R)-(1+a_0)\alpha_R\sinh^2\alpha_R]}{2\alpha_R+\sinh 2\alpha_R}, \tag{5a}$$

$$A_1=-\frac{Ka_1\operatorname{sech}\alpha_R}{4}, \tag{5b}$$

$$B_1=-Kb_1+\frac{Ka_1\coth 2\alpha_R\sinh\alpha_R}{2}, \tag{5c}$$

$$D_0=-\frac{A_0\cosh\alpha_R+Kb_0}{\alpha_R\sinh\alpha_R}, \tag{5d}$$

$$\frac{A_n}{K}=\frac{(n+1)-e^{-2n\alpha_R}-ne^{-2\alpha_R}}{n(n+1)[n\sinh 2\alpha_R+\sinh 2n\alpha_R]}, \tag{5e}$$

$$\frac{B_n}{K}=\frac{(n-1)+e^{-2n\alpha_R}-ne^{2\alpha_R}}{n(n-1)[n\sinh 2\alpha_R+\sinh 2n\alpha_R]}. \tag{5f}$$

And

$$K=-4R\omega\alpha_R\sinh\alpha_R[2S(2\alpha_R+\sinh 2\alpha_R)+4\alpha_R(a_0+1)\sinh^2\alpha_R-4b_0(\sinh\alpha_R+\alpha_R\cosh\alpha_R)-2b_1(2\alpha_R+\sinh 2\alpha_R)+a_1(2\alpha_R\coth 2\alpha_R\sinh\alpha_R-\alpha_R\operatorname{sech}\alpha_R-\tfrac{3}{2}\sinh\alpha_R+\tfrac{1}{2}\sinh 3\alpha_R)]^{-1}, \tag{6}$$

with all coefficients a_i, and b_i being evaluated at α_R; and

$$S=-\frac{A_0+A_1+B_1}{K}=\sum_{n=2}^{\infty}\frac{(-2n)e^{-2n\alpha_R}+(n-n^2)e^{-2\alpha_R}+(n+n^2)e^{2\alpha_R}}{n(n-1)(n+1)(n\sinh 2\alpha_R+\sinh 2n\alpha_R)}. \tag{7}$$

The accuracy of the solution depends on the summation S, and implicitly on the numbers of terms considered, which guarantees a value of n for the desired level of precision on the stream function. Whenever α_R values are small—large cylinders' radii VS gap—the number of terms required for the summation [Eq. (7)] increases. All parameters presented here were obtained with 125 terms assuring good accuracy over the complete flow domain.

III. THE FIELD PARAMETER AND THE SHEAR RATE

Despite the flow field being linear, it is not homogeneous. Four-roll mills[5] show that purely hyperbolic stream lines at the stagnation point are possible only if four vortices are present at points along the cardinal directions. Consequently, for the two-roll mill with two vortices explicitly associated with the cylinders, the remaining nonassociated vortices are located along the x axis. In order to characterize those features, the two most important observables of the strong flow field are the flow-type parameter λ, and the shear rate $\dot{\gamma}$. In particular, these parameters are most useful for studies of polymeric solutions, embedded objects, etc., over the extended stagnation region, where a well-characterized elongational flow exists. For λ, it is necessary to evaluate the magnitude of the rate of deformation $\|\mathbf{D}\|=\sqrt{\mathrm{Tr}(\mathbf{D}\mathbf{D}^T)}$ and the vorticity $\|\mathbf{W}\|$ as a function of position, taking into consideration an objective measure of vorticity. For $\dot{\gamma}$, the magnitude of the velocity gradient is needed. The flow-type parameter is

$$\lambda=\frac{\|\mathbf{D}\|+\|\overline{\mathbf{W}}\|}{\|\mathbf{D}\|-\|\overline{\mathbf{W}}\|}=\frac{|q|-|A|}{|q|+|A|}; \tag{8}$$

for $\alpha=0$ (the line between the cylinders),

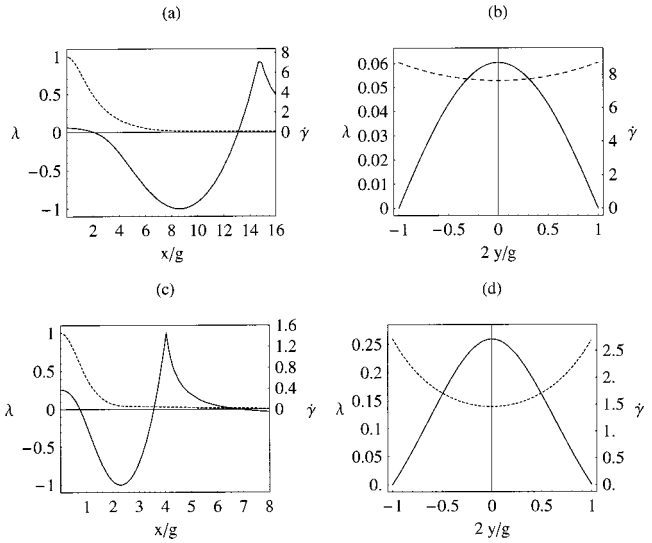

FIG. 1. Plots of flow-type parameter λ (solid lines) and the shear rate $\dot{\gamma}$ (dashed lines) along the *x* axis and the *y* axis normalized by half the gap distance. For rollers D (a) along the *x* axis and (c) for the *y* axis. For rollers I equivalent plots (b) and (d), respectively.

$$q=\frac{(B+C)}{h}+D, \quad B=\frac{\partial u_\alpha}{\partial \beta}, \quad C=\frac{\partial u_\beta}{\partial \alpha}, \quad D=\frac{\sin\beta}{d}u_\alpha, \tag{9a}$$

$$A=\frac{(B-C)}{h}+D-\frac{u_\alpha}{hq}\frac{\partial p}{\partial \alpha}, \tag{9b}$$

$$\frac{\partial p}{\partial \alpha}=\frac{1}{h}\left(\frac{\partial^2 u_\alpha}{\partial \alpha^2}-\frac{\partial^2 u_\beta}{\partial \alpha \partial \beta}\right)-\frac{\sin\beta}{d}C+\frac{u_\alpha}{d}; \tag{9c}$$

and for $\beta=\pi$—the line joining the axes of the cylinders—the coefficients are given by

$$q=\frac{(C+B)}{h}+D, \quad B=\frac{\partial u_\beta}{\partial \alpha}, \quad C=\frac{\partial u_\alpha}{\partial \beta}, \quad D=\frac{\sinh\alpha}{d}u_\beta, \tag{10a}$$

$$A=\frac{(C-B)}{h}-D-\frac{\mu_\beta}{hq}\frac{\partial p}{\partial \beta}, \tag{10b}$$

$$\frac{\partial p}{\partial \beta}=\frac{1}{h}\left(\frac{\partial^2 u_\alpha}{\partial \alpha \partial \beta}-\frac{\partial^2 u_\beta}{\partial \beta^2}\right)+\frac{\sinh\alpha}{d}C+\frac{u_\beta}{d}. \tag{10c}$$

The magnitude of the velocity gradient tensor, $\dot{\gamma}=\|\nabla \mathbf{u}\|$ is given by

$$\dot{\gamma}=\sqrt{\left(\frac{1}{h}B\right)^2+\left(\frac{1}{h}C+D\right)^2}. \tag{11}$$

Based on Eqs. (8) and (11), Fig. 1 shows $\dot{\gamma}$ and λ along the *x* and *y* axes normalized with respect to the gap, for two geometries that correspond to rollers D and I of Table I. The behavior is the same for all geometries, up to rollers with a λ value as high as 0.801. While $\dot{\gamma}$ (dashed lines) decays monotonically, λ (solid lines) has a positive value at the origin, decreases to a value close to -1 (due to a nonassociated vortex), sharply increases up to a value near one, followed by a slow monotonic decay to a value for $\lambda(x\to\infty)$ close to -1. In Fig. 1, the rotational speed of the cylinders is the same; consequently, the maximum shear rate depends on the gap width. Figures 1(b) and 1(d) present the typical spatial dependence along the line joining the centers of the cylinders ($\beta=\pi$). For λ the profile is almost parabolic. The values of $\dot{\gamma}$ across the gap have a flatter profile, especially for the smaller gaps.

For studies of complex fluids subjected to strong flows, the extent of the stagnation region can be defined up to the point where λ changes sign. The shear rate provides a second criterion for such a region based upon material points which separate at a constant rate. For smaller gaps the length of these regions is about 4.8 gap units regardless of the criteria, while for the largest gaps ($g=1.163R$) the extent of the region is smaller for a λ—than a $\dot{\gamma}$—criterion: 0.72 and 0.86 gap units, respectively.

Also, the impact of nonassociated vortices on the flow field depends on the geometry, being most relevant when the shear rate of the vortex is largest. Figures 1(a) and 1(c) show that the relative magnitude of $\dot{\gamma}$ at the vortices is higher for the largest λ values. Furthermore, the position along the *x* axis of the nonassociated vortices (where $\lambda=-1$) varies according to the λ value of the flow device. For the smallest gaps, the vortices are driven away to about twice the distance than that along the *y* axis to the center of rotation of the cylinder, and simultaneously their strength decreases. For the largest λ's available, the vortex position is about 5/3 the distance to the center of the cylinders; only for λ's close to 1 do the vortices' positions approach the distance to the cylinders axes.[14]

IV. EXPERIMENTAL, NUMERICAL, AND STOKES' SOLUTION RESULTS

Two-roll mill flow devices have been used in the past, especially to study polymeric fluids (e.g., Refs. 1, 2, and 15). In these studies, the centers of the cylinders are fixed 0.0170 m apart (on the *y* axis and measured from the center), and λ is varied using eight different sets of rollers. Columns 1–3 of Table I list the rollers' identification (from A to I), the cylinders' diameters, and the calculated value for *d*, associated with the origins of the radial vector of the bipolar coordinate system. Columns 4–6 of Table I present the values of λ, determined first by Eqs. (2)–(7), then the numerical value reported by Singh and Leal,[2] and finally the experimental values by Wang *et al.*[15] Entries without values in the numerical and experimental columns imply that these are not available. The magnitude of the velocity gradient at the stagnation point is also a function of its geometry via the tangential speed and the gap between rollers. Columns 7 and 8 provide information about $\dot{\gamma}/\omega$ by theoretical and experimental values ($[\dot{\gamma}/\omega]_{\text{expt}}$).

The experimental values are slightly higher than the numerical and theoretical predictions for λ and $\dot{\gamma}$, because different models of the flow field were used. As shown in Fig. 2(a), the numerical and experimental results have used a two-roll mill contained inside a third stationary, circular cylinder; a distortion of the unbounded fluid domain. However for rollers C to G, the theoretical values for λ and $\dot{\gamma}$ appear at odds with the experimental values but less with the numeri-

TABLE I. Dimensions for the two-roll mill with different diameters for the cylinders and their associated flow parameters. The cylinders' radii and the corresponding d values for the calculation of the Fourier series expansions are given in columns 2 and 3. For all cases, the distance between rollers' axes is fixed at 17.0 mm. The values of λ, evaluated at the stagnation point, are carried out using Eq. (2) with $n=125$. λ_{num} and λ_{expt} are the corresponding numerical and experimental results reported in Refs. 2 and 15, respectively. The right-most columns present the magnitude of the principal eigenvalue of the velocity gradient tensor, normalized with respect to the angular speed of the cylinders. $[\dot{\gamma}/\omega]$ is the theoretical value for the shear rate; and $[\dot{\gamma}/\omega]_{expt}$ is the reported result of Wang *et al.* (Ref. 15).

Rollers	Radii (mm)	d (mm)	λ ($n=125$)	λ_{num}	λ_{expt}	$\frac{\dot{\gamma}}{\omega}$	$\left[\frac{\dot{\gamma}}{\omega}\right]_{expt}$
A	16.65	3.431 836	0.010 437	···	···	47.239 90	···
B	16.35	4.655 910	0.019 620	···	···	24.823 93	24.1
C	15.70	6.519 969	0.040 316	···	0.047	11.750 69	11.7
D	15.10	7.809 609	0.060 461	···	0.067	7.624 681	7.84
E	14.17	9.392 076	0.094 123	···	0.096	4.690 372	4.83
F	14.00	9.643 651	0.100 692	···	0.114	4.351 319	4.44
G	12.78	11.210 334	0.152 789	0.153	0.160	2.727 231	2.80
H	11.69	12.342 767	0.207 191	···	0.196	1.919 587	1.84
I	10.75	13.169 567	0.259 108	···	···	1.457 431	···

cal results. The source of the discrepancy is not clear, but perhaps these results can provide some insight into the accuracy of the experimental technique or can be used as a benchmark to ''fine-tune'' the experimental measurements.

For rollers H, the marked drop of the measured values may be the result of significant three-dimensionality flow effects due to a length-to-gap ratio of about two to one. Also, the flow field on the layers next to the flat covers must be similar to that of simple shear flow, which implies that the observed value of λ must depend upon the depth of the flow cell. Furthermore, the velocity field may also be weaker due to the proximity of the container walls generating a smaller shear rate. This three-dimensional effect may also have other consequences; in particular, at high $\dot{\gamma}$ the stability of the flow may be compromised.

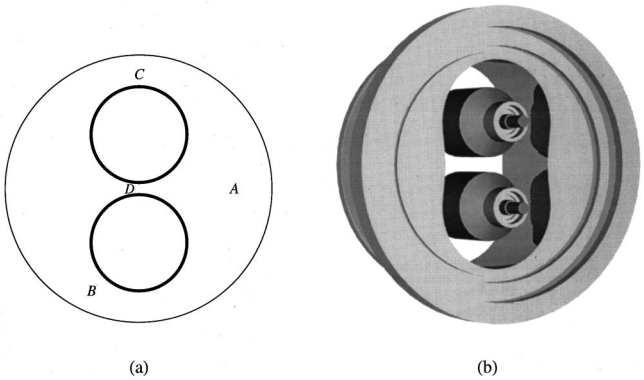

FIG. 2. Configuration of two-roll mills. (a) Mill reported in Refs. 1, 2, and 15: Region A represents a significant volume fraction of small relevance to the flow field. Region B presents a spurious elongational flow due to the existence of container walls. Region C can apply shear rates to the fluid microstructure as large as those generated in the central region. (b) The new container based on the streamlines calculated with the analytical solution. The flow cell also considers a cooling loop to maintain the temperature within 0.01 K. The top and bottom covers can be made of transparent crystal, allowing studies over the complete flow field. The rollers have conical ends to guarantee smaller shear rates for every fluid parcel than those applied at the stagnation point.

V. EXPERIMENTAL DEVICES FOR PLANAR, ELONGATIONAL FLOWS

Figure 2 shows a new flow cell based upon the calculated streamlines, and the typical two-roll mill configuration used to date with (1) region A representing a volume of fluid not used, (2) region B a secondary elongational flow domain since $\mathbf{u}\cdot\nabla\mathbf{u}\neq\mathbf{0}$, and (3) region C where shear rates can be of the same order as those that occur at the stagnation point, when the interior gap and that due to the presence of the walls have about the same width. Figure 2(b) shows the new flow cell exterior contour. Although the optimal location of the boundary on the $\alpha\beta$ plane may imply different effects on different flow properties, a general criterion is outlined which reduces the most important disadvantages mentioned above, and at the same time provide an estimate of the boundary's perturbation on the velocity field, λ, $\dot{\gamma}$, and the streamlines. The new contour for the container is based upon the calculated streamlines, assuming that the cylinders remain fixed as shown in Fig. 2(b). First, the range of geometries to be used defines the extreme variation on streamlines generated by a complete set of pairs of cylinders; see Fig. 3(a). The streamlines shown correspond to those of the largest and smallest diameters of cylinders in Table I. Second, the difference of areas—their absolute values along the streamline—delimited by these two streamlines is evaluated as a function of the distance away from the cylinders. For large radial distances away from a cylinder, the contours are very similar—at infinity, both streamlines are circles—but the length of the curve increases; closest to the cylinders, the area difference increases. Hence, there is a radial distance where the difference of the areas attains its minimum value. For a distance of 41.5 mm from a cylinder axis, the relative areal difference with respect to the total area contained within a closed streamline is less that 0.001. This curve will induce a small perturbation to all possible geometries of the two-roll mill and for the most relevant flow parameters.

Figures 3(b) and 3(c) present isopleths for the magnitude of the velocity field, $\|\mathbf{u}\|$, and $\dot{\gamma}$ for the overall domain with

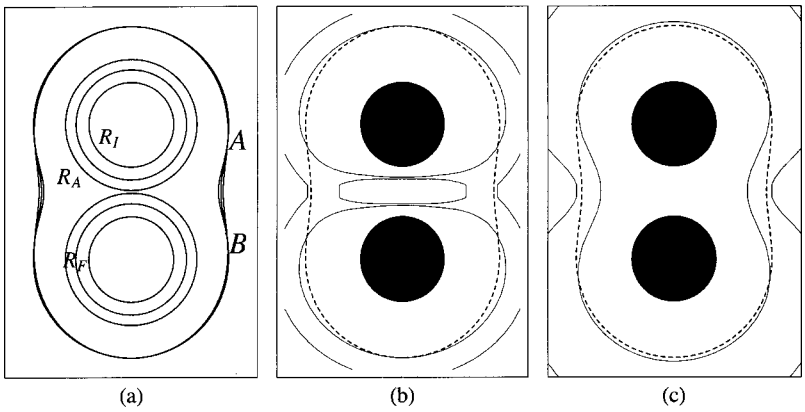

FIG. 3. The new container for two-roll mills is defined taking into account the distance at which the associated streamlines for the smallest and largest two-roll mills produce the minimum mismatch. (a) The optimum location minimizes the difference of the areas delimited by the streamlines associated to every mill. For rollers I, isopleths of the magnitude of the velocity field (b), and the velocity gradient (c) of the *unbounded* two-roll mill superposed by the contour—dashed line—of the flow cell.

the selected cell-contour superposed. For the magnitude of the fluid velocities, the most significant perturbation occurs on the portion of the flow furthest to the stagnation point (toward the exterior part of the cylinders), thus a minimal flow modification should be caused on parameters such as λ, the magnitude of the rate of deformation, and the objective vorticity. For isopleths of $\dot{\gamma}$, the strongest deviation occurs for the largest λ values near the $\alpha=0$ axis. However, these effects can be considered minimal because shear rates near the x axis and away from the stagnation point are already very small. Also for all those geometries, the rate of deformation is significantly larger at the stagnation point than far away. The variation of $\dot{\gamma}$ as a function of position along the selected streamline should increase most significantly opposite to the stagnation point behind the cylinders, where the relative modification can be at most 8% with respect to those generated at the stagnation point; furthermore, there should be a small change for the local values of λ. Finally, the machining of the walls with the prescribed streamline is possible if a sixth-order spline fit to the exterior wall is used. There are computer packages that generate the machining codes to the required precision.

VI. CONCLUSIONS

The use of the Fourier series solution for the Stokes flow generated by a two-roll mill can provide detailed information about a complete class of elongational flow with vorticity.[10] The solution presented here shows a good correlation among predicted values and the available experimental and numerical results for two of the most important flow parameters: the shear rate and the flow-type parameter. The solution is used to design and construct laboratory models of these flows that assure minimal perturbation to the desirable features of the flow. The elongational flows generated have characteristics defined exclusively by the geometry of the device and the rate of rotation of the cylinders. Furthermore, the analytical solution for these flows include the effects of inner boundaries. Because of the presence of the container's boundaries, a quantitative analysis of the perturbations is given for the velocity fields, the magnitude of the velocity gradient, the flow-type parameter, and the shear rate. These may be important advantages for studies of the microstructure of complex fluids, with analytical means to determine most of the effects due to creeping flows.

ACKNOWLEDGMENTS

Our special thanks to Gerardo F. Guevara and Jesús Camacho at the Materials Research Institute, UNAM. M.A.H.R. was supported by a DGEP-UNAM Scholarship. E.G. acknowledges partial support from Grants Nos. 3451A9310 and G27837U of CONACyT, IN303093 of PAPITT-DGAPA, UNAM, and 0598 of FIES-IMP.

[1] E. Geffroy and L. G. Leal, ''Flow birefringence studies of a concentrated polystyrene solution in a two-roll mill. I. Steady flow and start-up of steady flow,'' J. Polym. Sci., Part B: Polym. Phys. **30**, 1329 (1992).
[2] P. Singh and L. G. Leal, ''Computational studies of the FENE dumbbell model with conformation-dependent friction in a corotating two-roll mill,'' J. Non-Newtonian Fluid Mech. **67**, 137 (1996).
[3] S. C. Jana, G. Metcalfe, and J. M. Ottino, ''Experimental and computational studies of mixing in complex Stokes: The vortex mixing flow and multicellular cavity flows,'' J. Fluid Mech. **269**, 199 (1994).
[4] T. Atobe, ''Lagrangian chaos in the Stokes flow between two-eccentric rotating cylinders,'' Int. J. Bifurcation Chaos Appl. Sci. Eng. **7**, 1007 (1997).
[5] B. J. Bentley and L. G. Leal, ''An experimental investigation of drop deformation and breakup in steady two-dimensional linear flows,'' J. Fluid Mech. **167**, 241 (1986).
[6] H. A. Stone, ''Dynamics of drop deformation and breakup in viscous fluids,'' Annu. Rev. Fluid Mech. **26**, 65 (1994).
[7] R. R. Huilgol and N. Phan-Thien, *The Fluid Mechanics of Viscoelasticity* (Elsevier, Amsterdam, 1998).
[8] W. L. Olbricht, J. M. Rallison, and L. G. Leal, ''Strong flow criteria based on microstructure deformation,'' J. Non-Newtonian Fluid Mech. **10**, 291 (1982).
[9] M. S. Chong, A. E. Perry, and B. J. Cantwell, ''A general classification of three dimensional flow fields,'' Phys. Fluids A **2**, 765 (1990).
[10] M. A. H. Reyes and E. Geffroy, ''Study of low Reynolds number hydrodynamics generated by symmetric corotating two-roll mills,'' Rev. Mex. Fis. **46**, 135 (2000).
[11] J. Happel and H. Brenner, *Low Reynolds Number Hydrodynamics* (Kluwer, Dordrecht, 1991), pp. 497–499.
[12] G. B. Jeffery, ''The rotation of two-circular cylinders in a viscous fluid,'' Proc. R. Soc. London, Ser. A **101**, 169 (1922).
[13] C. Pozrikidis, *Theoretical and Numerical Fluid Mechanics* (Oxford University Press, Oxford, 1994).
[14] G. G. Fuller, J. M. Rallison, R. L. Schmidt, and L. G. Leal, ''The measurement of velocity gradients in laminar flows by homodyne-light scattering spectroscopy,'' J. Fluid Mech. **100**, 555 (1980).
[15] J. J. Wang, D. Yavich, and L. G. Leal, ''Time resolved velocity gradient and optical anisotropy in linear flows by photon correlation spectroscopy,'' Phys. Fluids **6**, 3519 (1994).